Vibrationally resolved carbon core excitations in alkane molecules

G. Remmers, M. Domke, and G. Kaindl
Institut für Experimentalphysik, Freie Universität Berlin, Arnimallee 14, W-1000 Berlin 33, Germany
(Received 2 November 1992)

Core-excitation spectra at the carbon K threshold of methane, ethane, and propane, as well as of the deuterated molecules, were studied by high-resolution photoabsorption using synchrotron radiation from the SX700/II monochromator at BESSY. The spectra contain signals from excitations to C $1s^{-1}np$ Rydberg states and their vibrational substates, as well as from transitions to C $1s^{-1}ns$ Rydberg states. The latter excitation is dipole forbidden in methane, but rendered possible by strong vibronic coupling. Transitions to vibrational substates could be identified via the observed isotope effects. The C $1s^{-1}np$ Rydberg states were found to be split by a Jahn-Teller effect or by molecular-field interaction. C-H and C-C equilibrium distances as well as vibrational frequencies in the core-excited molecular states were derived within the Franck-Condon model from the vibrational fine structures of the C $1s^{-1}3p$ Rydberg excitations.

PACS number(s): 33.20.Rm, 33.80.Rv, 35.20.Pa, 31.30.−i

I. INTRODUCTION

During the past few years, carbon $1s$ excitation spectra of a series of organic molecules have been thoroughly investigated, with the emphasis put on molecules with π-bonded electrons, which give rise to strong excitations into long-lived π^* resonances. Much less frequent are studies of core-excitation spectra of the simplest hydrocarbons, the alkanes (C_xH_{2x+2}), most of which were additionally performed with rather moderate resolution [$\cong$600 meV, (FWHM)] using inner-shell electron-energy-loss spectroscopy (ISEELS) [1–4]. Only in the case of CH_4, could some fine structure due to vibrational excitations be resolved by ISEELS [5,6]. High-resolution photoabsorption using synchrotron radiation is a suitable technique for providing related results, however, with much better statistical accuracy and—very recently—also with substantially improved energy resolution [7–10]. Even though a high-resolution photoabsorption study of a saturated hydrocarbon, ethane, was recently reported [9], a systematic investigation of the fine structure of the excitation spectra across the series of alkane molecules (methane, ethane, propane) is still missing.

In this paper, we report on a high-resolution photoabsorption study of the C $1s^{-1}$ core excitation spectra of the first three alkanes, methane, ethane, and propane, as well as of their deuterated forms. Transitions to vibrationally excited states were identified by isotropic replacement on the basis of the observed isotope effects. Dipole-forbidden transitions were observed and explained assuming vibronic coupling. A Franck-Condon analysis of the C $1s^{-1}3p$ excitation spectra resulted in vibrational frequencies and equilibrium distances for the C $1s$ core-excited molecules.

II. EXPERIMENT

The measurements were performed with the high-resolution SX700/II monochromator, operated by the Freie Universität Berlin at the Berliner Elektronenspeicherring für Synchrotronstrahlung (BESSY) [8]. Using a recently installed 2442-line/mm grating, a resolution of $\cong$60 meV (FWHM) at the C K threshold ($h\nu\cong$290 eV) was obtained [11]. The photon energy was calibrated via the C $1s^{-1}\pi^*$, $v'=0$ state of carbon monoxide (CO) at 287.400 eV. Since the SX700/II monochromator has no entrance slit, even small changes in the vertical position of the stored electron beam will affect the energy calibration, causing shifts up to 200 meV at $h\nu=290$ eV between different injections. This was taken into account by repeated calibration runs with CO as well as with the alkanes, leading to a *relative* energy calibration of ±2 meV; absolute energies are not better defined than ±20 meV.

Photoemission spectra were taken with an ionization chamber of 10-cm active length by recording the total ionization current as a function of photon energy. The chamber was filled with methane, ethane, and propane, respectively, at pressures of $\cong$0.1 mbar, and separated from the UHV monochromator by a 1500-Å-thick Al (1 at.% Si) window. Saturation effects are negligible for the studied gas pressures; for pressures higher than $\cong$0.5 mbar, however, the most intense spectral features were found to show broadening due to saturation.

III. C $1s^{-1}$ RYDBERG TRANSITIONS

A. Methane

The C $1s^{-1}$ core-excitation spectra of methane, CH_4 and CD_4, are presented in Fig. 1. These spectra show resonance excitations into Rydberg states close to the C K threshold as well as into vibrational substrates. For an unambiguous assignment of these resonances, it is very helpful to compare the CH_4 and CD_4 spectra, since substantial shifts in energy upon deuteration are only expected for vibrational substates. For the five-atom molecule methane, nine normal vibrational modes are possible.

Degeneracies of these vibrational frequencies due to symmetry reduce the number of normal modes to four. These are a single a_1 mode, a single e mode, and two modes with t_2 symmetry. In photoabsorption, the number of observable modes can be further reduced due to the dipole selection rules.

The spectra in Fig. 1 are dominated by a resonance at 287.98 eV, which is attributed to a C $1s \rightarrow 3p$ transition [3–5], representing the lowest dipole-allowed C $1s^{-1}$ excitation. However, at even lower energies (at 287.03 eV in the case of CH_4 and at 286.99 eV in the case of CD_4), weaker resonances are visible, the most intense of which had been observed before by ISEELS [2–4,6] as well as by low-resolution photoabsorption [12–14]. They are assigned to dipole-forbidden C $1s \rightarrow 3s$ transitions rendered possible by vibronic coupling (see discussion further below). Due to the substantially improved resolution and spectral noise, satellites of this resonance are clearly observable here, at 286.82 eV and 287.42 eV in the case of CH_4, and at 287.21 eV in the case of CD_4. It should be noted that the excitation of the adiabatic C $1s \rightarrow 3s$ transition from the ground state ($v''=0$) into the ground-vibrational $1s^{-1}3s$ state ($v'=0$) is forbidden, even in the case of very strong vibronic coupling. This means that all of the observed C $1s^{-1}3s$ features must be due to excitations into antisymmetric vibrational substates.

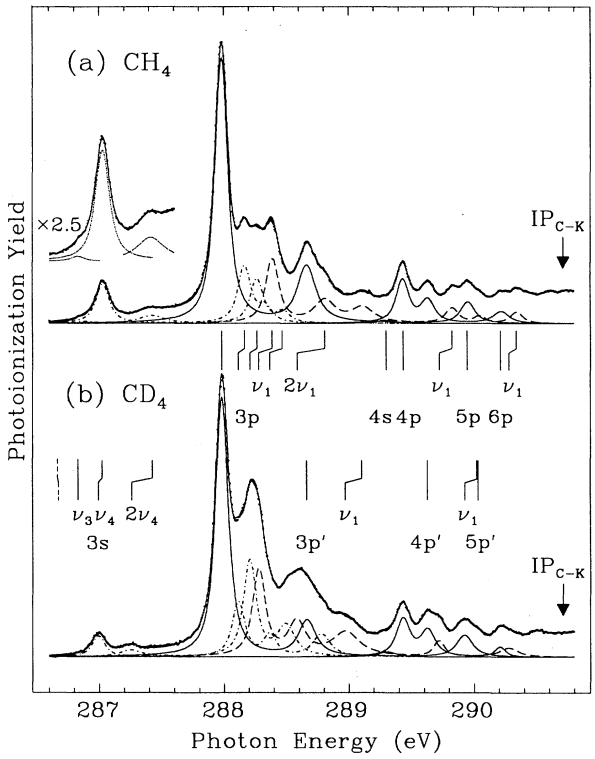

FIG. 1. High-resolution C $1s^{-1}$ photoionization spectra of (a) CH_4 and (b) CD_4. The solid lines through the data points are the results of least-squares fits with Lorentzian lines convoluted by a Gaussian (Voigt profile) to simulate finite experimental resolution. The solid subspectra represent ground-vibrational (adibatic) Rydberg transitions, while the dashed subspectra denote the respective ν_1 vibrations (symmetric C-H stretching mode); the dash-dotted subspectra are assigned to ν_2, ν_3, and ν_4 vibrations, excited due to vibronic coupling. The solid vertical bars mark the positions of the fitted resonances and indicate the isotope shifts upon deuteration. The dashed vertical bars indicate the positions of the derived hypothetical adiabatic C $1s^{-1}3s$ excitation. IP denotes ionization potential.

For an assignment of the higher Rydberg states and their vibrational substates, the spectra of undeuterated and deuterated methane are compared. It is apparent that the resonances in the range from 288.05 eV to 288.6 eV shift in energy upon deuteration, and are therefore excitations into vibrational substates of the dominant C $1s^{-1}3p$ line. On the other hand, the resonance at $h\nu=288.64$ eV does not shift, and is accordingly assigned to a transition into the ground-vibrational level of a separate Rydberg state (adiabatic transition).

A further helpful tool for the assignment of peaks is provided by the Rydberg formula, which defines the energy positions of individual transitions in a Rydberg series as a function of the ionization limit and the quantum defect. Applying this formula, quantum defects in the range from 1.0 to 1.2 for s states, 0.7 to 0.8 for p states, and ≤ 0.2 for d states, respectively, were found to reasonably describe Rydberg series in molecules. With the K ionization limit of methane at $\cong 290.7$ eV, the resonance at 288.64 eV leads to a quantum defect of 0.42, excluding an assignment of this peak as an s or d state. Instead, its origin due to Jahn-Teller splitting of the degenerate $3p(^1T_2)$ state, caused by deviations from the ideal tetrahedral symmetry, is most probable [6]. According to a study of the Jahn-Teller effect in excited valence states of methane [15], any of the antisymmetric vibrational modes can serve as the active mode responsible for the distortions from the ground-state symmetry into D_{2d} or C_{3v} symmetry. However, the type of the symmetry-distorted mode is not known, and the states are consequently labeled as $3p'$. Note that this uncertainty in the symmetry of the np states does not lead to an ambiguity in the following symmetry considerations. Similar to the $3p$ resonance, the $3p'$ resonance is also accompanied by vibrational satellites up to an energy of $\cong 289.25$ eV.

The following resonance ($4p$) is analogously split into $4p$ and $4p'$ states at 289.43 eV and 289.63 eV, respectively, which are again accompanied by $4p$ vibrational satellites at 289.82 eV (CH_4) and 289.72 eV (CD_4). The Jahn-Teller splitting of the $4p$ state (200 meV) is naturally smaller than that of the $3p$ state (680 meV), since a Jahn-Teller distortion of the molecule will most strongly affect the innermost Rydberg states. In the case of the $5p$ state, represented by the resonance line at 289.93 eV, this splitting is further reduced, and the respective $5p'$ resonance is only noticeable as a shoulder of the main $5p$ peak at 290.0 eV; for CH_4, the $5p'$ resonance also overlaps with a vibrational satellite of the $4p'$ resonance. The assignment of an even higher Rydberg transition, the $6p$ resonance at 290.21 eV, is also given in Fig. 1. With the exception of the dominant C $1s^{-1}3p$ state, all other Rydberg states can be fitted quite well by assuming only a single vibrational mode with a vibrational energy of $\cong 400$ meV (250 meV) in the case of CH_4 (CD_4). For a detailed discussion

of the origin of the vibrational modes, see below.

In a recent configuration-interaction calculation of K-shell excited methane [16], the results of which were compared with the relatively low-resolution ISEELS data of Ref. [6], the $3p'$ resonance was assigned to the excitation of a second valence-Rydberg state with $^1T_2$ symmetry. This is in obvious disagreement with the present interpretation, where the $3p'$ resonance was assigned to a Jahn-Teller splitting of the C $1s^{-1}3p$ state. In view of the analogous splittings of the higher C $1s^{-1}4p$ and C $1s^{-1}5p$ states, which cannot be explained by the arguments given in Ref. [16], the presence of a Jahn-Teller splitting is most probable. It is, however, possible that both mechanisms contribute to the $3p'$ peak structure in the spectra of Fig. 1. A clarification has to wait for a detailed theoretical analysis of the present high-resolution spectra of CH_4 and CD_4.

B. Ethane

In Fig. 2, the C $1s^{-1}$ core-excitation spectra of ethane, C_2H_6 and C_2D_6, are shown. The eight-atom ethane molecule allows 12 different normal vibrational modes. Despite this general complexity, it turns out that essentially only two vibrational frequencies contribute to the spectra: the ν_1 vibrational attributed to a symmetric C-H stretching mode, and the ν_3 vibration representing a symmetric C-C stretching mode; these modes are denoted here in the usual way [17]. Other vibrational modes can be excited, but they apparently lead only to slight broadenings of the ν_1 and ν_3 vibrational satellites.

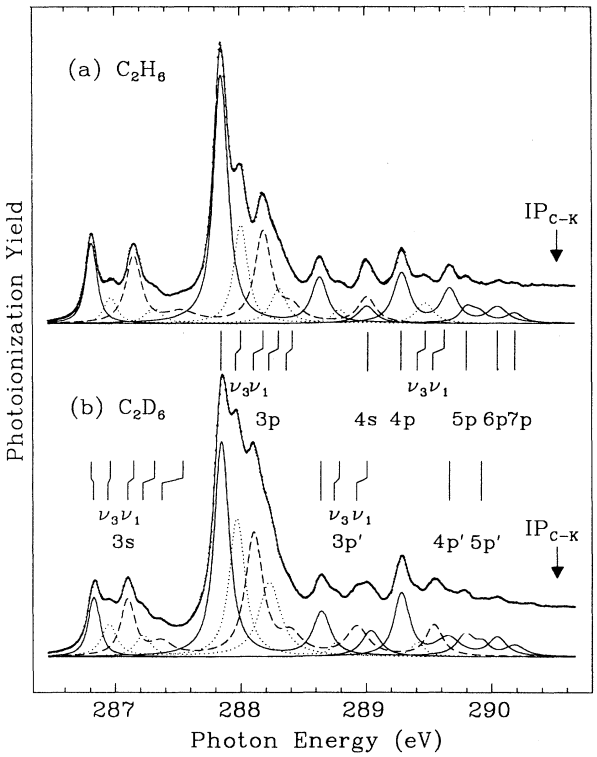

FIG. 2. High-resolution C $1s^{-1}$ photoionization spectra of (a) C_2H_6 and (b) C_2D_6. The solid lines through the data points are the results of least-squares fits with Voigt profiles. Solid subspectra: ground-vibrational (adiabatic) Rydberg transitions; dashed subspectra: ν_1 vibrations (symmetric C-H stretching mode); dotted subspectra: ν_3 vibrations (symmetric C-C stretching mode).

As in the case of methane, the dominant spectral feature is due to the C $1s^{-1}3p$ excitation, which is here at $h\nu=287.85$ eV. At lower energies, the C $1s^{-1}3s$ transition is observed at 286.82 eV, but with much higher spectral weight than in the methane case. This $3s$ resonance is accompanied by four partially resolved vibrational satellites at energies between 286.9 and 287.6 eV. Two vibrational series can be identified from their different energy separations and intensities: a high-energy vibration ν_1 (dashed subspectra), probably due to the symmetric C-H stretching mode, and a low-energy vibration ν_3 (dotted subspectra), probably due to the C-C stretching mode. Also, vibrations with frequencies $\nu_1+\nu_3$ and $\nu_1+2\nu_3$ are observed. This assignment is confirmed by comparison with the results for deuterated ethane: $\nu_1=330$ meV (260 meV) and $\nu_3=150$ meV (105 meV) for C_2H_6 (C_2D_6).

Analogous vibrational sidebands can also be identified in the case of the C $1s^{-1}3p$ state: a ν_3 vibrational satellite at 288.01 eV (287.96 eV) and a ν_1 vibrational substate at 288.19 eV (188.12 eV) for C_2H_6 (C_2D_6); the latter is accompanied by additional ν_3 and ν_1 vibrational excitations, respectively. Similar to the case of methane, a splitting of the $3p$ resonance is observed, with the $3p'$ resonance at 288.64 eV, but it is caused here by molecular-field interaction, which—due to the symmetry of the undisturbed molecule—gives rise to two resonances with E_g and A_{2u} symmetry, respectively. The $3p'$ state has also a ν_3 vibrational satellite at 288.80 eV (288.76 eV) and a ν_1 vibrational substate at 289.01 eV (288.92 eV) for C_2H_6 (C_2D_6). The C_2D_6 spectrum shows an additional resonance line at 289.03 eV, which is probably hidden in the $3p'$ ν_3 peak in the C_2H_6 spectrum; it is assigned to a $4s$ Rydberg state. The following peak at 289.29 eV is due to a $4p$ Rydberg state, accompanied by a ν_3 vibrational satellite at 289.47 eV (289.41 eV) as well as by a ν_1 vibrational satellite at 289.62 eV (289.54 eV) for C_2H_6 (C_2D_6). It is followed by a possible $4p'$ resonance due to molecular-field interaction. At 289.80 eV, the $5p$ resonance is observed, again with a $5p'$ satellite, followed by higher Rydberg resonances that can be identified up to $7p$ (see Fig. 2).

The present assignments are in close agreement with those given in Ref. [9], with the exception of the $3p'$ resonance, which was assigned there to a $3d$ Rydberg state; this is not supported, however, by its quantum defect of 0.34. Moreover, the spectrum of C_2D_6 given in Ref. [9] deviates substantially in the most intense spectral features from the one obtained here. From the present systematic studies, we can say that these differences arise from saturation effects, i.e., that the C_2D_6 spectrum in Ref. [9] resembles closely the saturated spectra recorded here for gas pressures higher than 0.5 mbar.

C. Propane

The C $1s^{-1}$ core-excitation spectra of propane, C_3H_8 and C_3D_8, are presented in Fig. 3. As in the case of methane and ethane, the spectra are dominated by the C $1s^{-1}3p$ transition at 287.68 eV, accompanied by rather intense vibrational satellites. In addition, the C $1s^{-1}3s$ state, and its vibrational substates, are observed in the energy range from 286.8 to 287.5 eV; transitions to this state and its vibrational satellites are much more intense than in methane and ethane. From a comparison of the spectra for undeuterated and deuterated propane, the following signals from adiabatic transitions to separate Rydberg states can be identified: a $3p'$ state at 288.61 eV, a $4p$ ($4p'$) state at 289.12 eV (289.50 eV), a $5p$ ($5p'$) state at 289.60 eV (289.70 eV), and a $6p$ state at 289.87 eV.

In a first approximation, the vibrational structure of most of the spectrum can be explained again by assuming contributions from only two vibrational modes out of a total of 27 possible modes [17]. Similar to the case of ethane, the $3s$ resonance is most likely accompanied by satellites due to a symmetric C-C stretching vibrational mode ν_8, a symmetric C-H stretching mode ν_3, as well as $\nu_8+\nu_3$ and $\nu_8+2\nu_3$ modes. Clearly resolved ν_8 and ν_3 vibrational modes are also observed for the $3p'$ and the $4p$ resonances. On the other hand, the dominant $3p$ excitation has a rather complex line profile due to overlapping vibrational satellites, which can no longer be described by only two contributing vibrational modes.

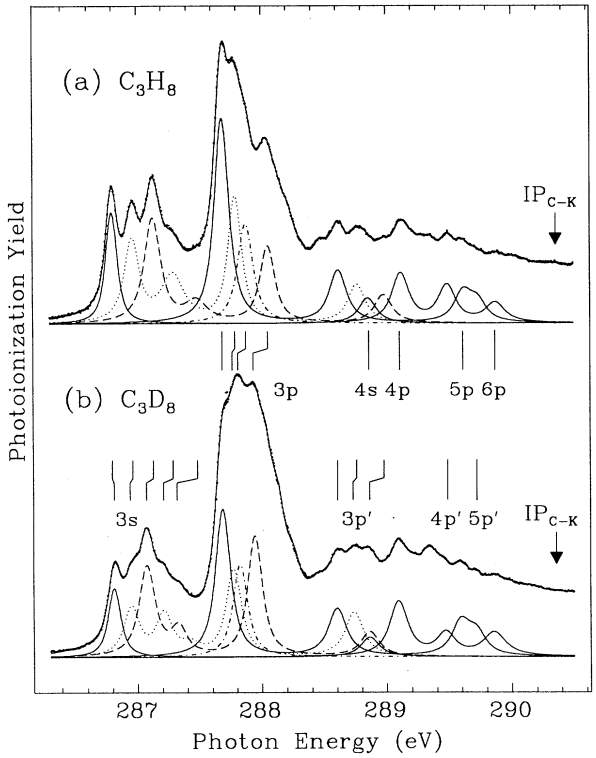

FIG. 3. High-resolution C $1s^{-1}$ photoionization spectra of (a) C_3H_8 and (b) C_3D_8, with the solid lines through the data points representing the results of least-squares fits with Voigt profiles. Solid subspectra: ground-vibrational (adiabatic) Rydberg transitions; dashed subspectra: $\nu_{2;3}$ vibrations (symmetric C-H stretching mode); dotted subspectra: ν_8 vibrations (symmetric C-C stretching mode); dash-dotted subspectra: $\nu_{4;6}$ vibrations (CH_3/CH_2 deformation mode). For reasons of clarity, the complete subspectra are shown only for the $3s$ excitations, whereas for the other excitations, the subspectra are only given for the lowest $\nu_x=1$ transition, with no other vibrations excited. In the fit analysis, however, the double vibrational excitations were fully taken into account.

IV. VIBRONIC COUPLING

Methane, ethane, and propane have T_d, D_{3d}, and C_{2v} symmetry, respectively, in their ground states. Only for methane, $1s\rightarrow 3s$ transitions are therefore strictly dipole forbidden, while they are dipole allowed for ethane and propane. In ethane, this is due to the interaction of the two C atoms causing a splitting of the C $1s$ states into states of a_{1g} and a_{2u} symmetry, respectively. The two states are almost degenerate, however.

In methane, a direct $1s\rightarrow 3s$ transition is dipole forbidden; a *dipole*-allowed transition to the C $1s^{-1}3s$ state is only possible if antisymmetric vibrational modes are excited that lead to a totally symmetric transition matrix element. The oscillator strength of such a transition is usually rather low, but can be considerably enhanced by mixing with an allowed electronic state of the same symmetry ("intensity borrowing"), if both resonances are less than $\cong 1$ eV apart [18]. However, for all forbidden electronic transitions observed due to vibronic interactions, the adiabatic transition (i.e., the transition from the ground state with $v''=0$ into the excited state with $v'=0$) is absent [19]. Hence, the spectral intensity of the methane C $1s\rightarrow 3s$ transition originates solely from excitations of the two antisymmetric t_2 vibrations. Considering the ground-state frequencies of these vibrations (ν_3: 162 meV (124 meV) and ν_4: 374 meV (280 meV) for CH_4 (CD_4) [16]), the energy separations between the two prominent $3s$ features in the spectra of Fig. 1 (380 meV and 260 meV in the case of CH_4 and CD_4, respectively) are close to the value of ν_4. Remember that slightly different vibrational energies are expected for the $1s^{-1}3s$ excited state. Hence, assuming the two distinct $1s^{-1}3s$ peaks to be ν_4 and $2\nu_4$ vibrational excitations, we estimate the position of the adiabatic line to be at 286.66 eV (286.69 eV) for CH_4 (CD_4). This assignment is confirmed by the shoulder at 286.82 eV in the spectrum of CH_4, which can be assigned to an excitation to the second t_2 vibrational mode ν_3. This leads to the same position of the adiabatic line. In the case of CD_4, both the intensity of the ν_3 mode and the energy separation between the ν_3 and ν_4 modes are too small to resolve the ν_3 mode in the measured spectrum.

Alternatively, the shoulder at 286.82 eV in the spectrum of CH_4 might be interpreted as the ground-vibrational adiabatic line of an electric *quadrupole* transition, since the $1s\rightarrow 3s$ transition is *dipole* forbidden but quadrupole allowed. This assignment, however, can be excluded, since then the other vibrational lines cannot be assigned in a consistent way; in particular, no isotope effect on the intensities of the observed lines should occur

in this case.

These assignments are further supported by the observed energy shift of the C $1s^{-1}3s$ adiabatic resonance upon deuteration. As discussed above, the adiabatic resonance energy increases slightly upon deuteration (dashed vertical bars in Fig. 1), even though the observed transitions to ν_4 and $2\nu_4$ vibrationally excited states shift to lower energies (solid bars in Fig. 1). Similar isotope shifts towards higher binding energies in the deuterated forms were also observed in the spectra of ethane and propane (see Figs. 2 and 3) as well as in the C $1s^{-1}3s$ excitation of formaldehyde [11]. These isotope effects can be explained by the sizes of the molecular orbitals interacting with the lowest Rydberg orbital. The effect is expected to be small for small molecules (and the thermal average C-H distance R_g in CD_4 is in fact, by $\cong 4$ mÅ, smaller than in CH_4), since the Rydberg electron will then be affected by a more completely screened potential, i.e., its energy will shift to higher values.

The C $1s^{-1}3s$ signal in the photoabsorption spectrum of methane is caused by vibronic coupling, which means that electronic and nuclear motion cannot be fully separated. If vibronic coupling occurs, a Franck-Condon analysis of the vibrational fine structure is no longer possible, since it would presume exactly such a separation. In addition, vibronic coupling leads to an isotope effect on the intensity of the dipole-forbidden C $1s^{-1}3s$ resonance signal, which is indeed more intense in CH_4 than in CD_4. The ratio of intensities of the C $1s^{-1}3s$ and the C $1s^{-1}3p$ resonances, $P = I^{3s}/I^{3p}$, both for CH_4 and CD_4, allows one to decide on the kind of coupling mechanism that gives rise to vibronic coupling, either Herzberg-Teller (HT) coupling or Born-Oppenheimer (BO) coupling [4,20]. HT coupling involves a dependence of the molecular electronic wave function on internuclear distance, while BO coupling assumes a complete violation of the Born-Oppenheimer approximation due to a nonvanishing nuclear momentum. It turns out that $P_D^{HT}/P_H^{HT} \propto \nu_D/\nu_H$ and $P_D^{BO}/P_H^{BO} \propto (\nu_D/\nu_H)^3$ for the two coupling mechanisms, respectively. Here the superscripts refer to the coupling mechanism, and ν are the respective vibrational frequencies, which change by a factor ranging between 0.71 and 0.77 upon deuteration [18]. Consequently, an intensity ratio of $P_D/P_H \cong 0.75$ will be characteristic for HT coupling, whereas ratios smaller than 0.5 are the effect of BO coupling. With moderate-resolution ISEELS, a ratio of $P_D/P_H = 0.81$ has been derived for methane, favoring HT coupling [4]. If all vibrational substrates of the $3s$ and $3p$ states are taken into account, as in the present work, the ratio decreases to 0.57 ± 0.05; it is consistent with predominant BO coupling.

In the case of ethane and propane, the intensity of the C $1s^{-1}3s$ adiabatic resonance signal increases to 20% and 50%, respectively, of the intensity of the C $1s^{-1}3p$ adiabatic excitation (to the lowest vibrational state with $v'=0$). No isotope effects on the intensities of the *adiabatic* transitions are observed, since vibronic coupling is not essential for this excitation. However, if again all vibrational substates are taken into account both for the C $1s^{-1}3s$ and the C $1s^{-1}3p$ excitation, an isotope effect is observed, with $P_D/P_H = 0.75 \pm 0.02$ (0.65 ± 0.02) for ethane (propane). It is due to the high spectral weight of transitions to the $3p$ vibrational substrates in the deuterated alkanes. These P_D/P_H ratios suggest therefore that the intensity of the C $1s^{-1}3s$ signal in ethane and propane is influenced by the HT coupling mechanism. In both molecules, the $1s \rightarrow 3s$ core excitation is not dipole forbidden, but a substantial fraction of the intensity originates from excitation of antisymmetric modes due to vibronic coupling. The frequencies of these antisymmetric vibrations differ only slightly from those of the symmetric modes; vibronic coupling leads therefore to increases in intensity and to line broadening of the C $1s^{-1}3s$ vibrational substrates, which can be best seen in the case of the C $1s^{-1}3s$ ν_1 vibrational states. The situation prevents a Franck-Condon analysis of the vibrational fine structure in this case.

A further consequence of vibronic coupling is the fact that more than one vibrational mode contributes to the fine structure of the C $1s^{-1}3p$ state in methane. These additional modes can also contribute to the $3p'$, $4p$, etc. resonances. For np states, the only dipole-allowed vibration is the totally symmetric ν_1 mode, with ground-state vibrational energies of 361.59 meV for CH_4 and 261.35 meV for CD_4 [19]. In the C $1s^{-1}3p$ excited state of CH_4 (CD_4), the most intense vibrational feature is in fact assigned to the ν_1 mode, with a vibrational energy of 420 meV (300 meV). The other vibrational substates of the C $1s^{-1}3p$ resonance originate from the vibrational modes ν_2, ν_3, and ν_4, which have ground-state vibrational energies in CH_4 (CD_4) of 190 meV (135 meV), 374 meV (280 meV), and 161 meV (123 meV), respectively. Due to the symmetry properties of the point group T_d, these modes gain intensity through the mixing of the respective vibronic states with the neighboring, dipole-allowed adiabatic $3p$ state. The vibrational energies of these forbidden vibrations in the core-excited $3p$ state are obtained from the spectra in Fig. 1 as 185 meV (133 meV), 284 meV (223 meV), and 495 meV (385 meV) for CH_4 (CD_4); they are therefore assigned to ν_4, ν_2, and ν_3 modes, respectively. Since the vibrational satellites of the $3p'$ resonance are substantially more intense in CD_4 than in CH_4, excitation of *two* vibrational quanta (ν_4 and ν_2) is observed in the spectrum of CD_4 at $h\nu = 288.75$ eV; the analogous feature cannot be identified in the spectrum of CH_4 due to lower intensity.

V. FRANCK-CONDON ANALYSIS

As we have seen, a Franck-Condon (FC) analysis of vibrational fine structure is only justified for symmetry-*allowed* vibrational substates of dipole-*allowed* transitions, which excludes all of the spectral features due to vibronic coupling. Consequently, the only core excitation accessible to FC analysis in the spectra of the alkane molecules is the C $1s^{-1}3p$ resonance with its a_1 vibrational satellites. At higher energies, where the $4p$, $5p$, etc. Rydberg states are observed, the additional split states ($3p'$, $4p'$, etc.) and their vibrational substates lead to considerable spectral overlaps, rendering FC fits rather ambiguous. In the FC analysis applied here, Morse potentials

were assumed for both the ground state and the excited molecular states. On the basis of the known internuclear distances and vibrational frequencies in the ground states, the respective values for the core-excited states are obtained.

Note that a FC analysis provides only *differences* in equilibrium intranuclear distances between ground state and excited states, but no absolute values. The ground-state frequencies are known with high precision for both the undeuterated and the deuterated alkanes [17]: upon deuteration, the vibrational frequencies decrease by factors ranging from 1.1 to $\sqrt{2}$, where the latter value is approximately observed for the "C-H" vibrational mode. On the other hand, equilibrium internuclear distances R_e are unknown for most multiatomic molecules. Instead, only zero-point vibrational level distances R_0, or thermal average values R_g, are known, which are usually quite different: for methane, e.g., $R_g = 1.1068$ Å [20], while $R_e = 1.058$ Å [21]. The R_g and R_0 values of methane decrease by 4 mÅ and 2 mÅ, respectively, upon deuteration, whereas the R_e values of CH_4 and CD_4 are almost the same, differing by only 0.1 mÅ [21]. Similarly, the R_g and R_0 values of ethane, both for C-H and C-C, decrease upon deuteration by 5 mÅ and 2 mÅ, respectively, with no R_e values known. In the case of propane, internuclear distances are only known for undeuterated C_3H_8. We conclude from these results from the literature that the equilibrium internuclear distances in the ground states of the alkane molecules exhibit almost no changes upon deuteration.

The only dipole-allowed transitions to vibrational substates occur to those with a_1 symmetry. In the case of methane, only the ν_1 vibrational mode has a_1 symmetry. Since vibrational modes of different symmetry cannot mix, a single-mode FC fit analysis can be applied here. In the case of ethane, three vibrational modes possess a_1 symmetry: the ν_1 mode (C-H stretching), the ν_2 mode (C-H_2 deformation), and the ν_3 mode (C-C stretching). In order to take these three modes into account, a multimode FC analysis becomes necessary. This requires a normal-mode analysis of the molecular vibrations in order to correlate the internuclear distances and bond angles with the normal vibrational frequencies, which are related to the observed vibrational frequencies. A complete treatment has to take into account all of the different bond lengths, molecular angles, and force constants, leading to systems of (19×19) matrices. Using an approximation that neglects the interaction of the two CH_2 groups of ethane, and applying symmetry arguments [22], the analysis is considerably simplified. In the case of propane, eight out of 27 possible vibrational modes possess a_1 symmetry, but a sufficient FC fit analysis can be performed with only three independent modes, one of the modes ν_2 or ν_3, one of the modes ν_4 or ν_6, and ν_8. Since ground-state anharmonicities are not known, they could not be taken into account in all of the studied cases. The results of this FC fit analysis are summarized in Table I: the ground-state distances assumed for ethane and propane deviate slightly from the minima R_e of the Morse potentials (see above).

A close inspection of Table I shows that—in analogy to the ground states—deuteration of the alkanes leads to lower vibrational frequencies in the C $1s^{-1}3p$ state, but to only small differences in the equilibrium internuclear distances. As a consequence, the intensities of the vibrational substates are much higher in the deuterated alkanes, with the consequence that higher vibrational modes are more likely to be excited. On the other hand, this complicates the analysis of the spectra of the deuterated alkanes due to overlaps between the vibrational substates, and in this way increases the error bars, particularly in the case of C_3D_8.

The only significant change in internuclear distance in the C $1s^{-1}3p$ states upon deuteration is found for methane. Here, the equilibrium C-D distance in the core-*excited* state of CD_4 is 19 mÅ larger than in CH_4. This is similar to the case of H_2CO [11], where an increase by 54 mÅ was found for the C $1s^{-1}\pi^*$ state upon

TABLE I. Equilibrium bond lengths R (in Å), and vibrational energies $h\nu$ (in meV), for the main totally symmetric vibrational modes in the ground state (g.s.) and the core-excited C $1s^{-1}3p$ state of CH_4, CD_4, C_2H_6, C_2D_6, C_3H_8, and C_3D_8. For the ground-state values, see text. Error bars are given in parentheses in units of the last digit.

		$R_{C\text{-}H(D)}$	$R_{C\text{-}C}$	$h\nu_1$	$h\nu_2$	$h\nu_3$
CH_4	g.s.	1.085		361.59		
	C $1s^{-1}3p$	0.996(3)		424(5)		
CD_4	g.s.	1.085		261.35		
	C $1s^{-1}3p$	1.015(3)		301(5)		
C_2H_6	g.s.	1.095	1.534	366.21	172.13	123.33
	C $1s^{-1}3p$	1.156(3)	1.5412(3)	344(5)	164(5)	156(3)
C_2D_6	g.s.	1.095	1.534	258.25	143.13	104.5
	C $1s^{-1}3p$	1.161(6)	1.554(3)	266(5)	143(5)	106(8)
				$h\nu_{2;3}$	$h\nu_8$	$h\nu_{4;6}$
C_3H_8	g.s.	1.095	1.526	360	107.6	$\cong 180$
	C $1s^{-1}3p$	1.005(3)	1.453(4)	364(5)	104(5)	184(9)
C_3D_8	g.s.	1.095	1.526	258	88.3	134
	C $1s^{-1}3p$	0.996(5)	1.456(4)	259(10)	81(10)	138(6)

deuteration. In the case of ethane and propane, no changes in internuclear distances were found within the limits of error. The large sizes of these two molecules obviously suppress measurable effects due to deuteration.

We can also compare the present results for the internuclear distances with those of zero-kinetic-energy photoemission studies, where vibrational sidebands beyond the carbon K threshold were observed and analyzed in a FC picture [23]. In this work, the difference in C-H distance between the ground state of CH_4 and the CH_4^+ photoionized state was reported to be -52 mÅ, i.e., slightly smaller than the respective values of -90 mÅ and -70 mÅ found here for the *core-excited* C $1s^{-1}3p$ states in CH_4 and CD_4, respectively. We can say that there is qualitative agreement between the results of the zero-kinetic-energy photoemission study of methane and the present observations.

VI. SYSTEMATIC TRENDS WITHIN THE ALKANE SERIES

In summary, we shall point out some systematic trends observed for the alkane series, i.e., when going from methane via ethane to propane.

(i) We first note that the Jahn-Teller splitting of the C $1s^{-1}3p$ state in CH_4 has a value of 660 meV. The respective value of the molecular-field splitting in C_2H_6 increases to 790 meV, and further to 930 meV in C_3H_8. This trend can be explained by the increasing sizes of the molecules and increasing disturbance on the Rydberg states.

(ii) The mechanism of vibronic coupling changes from approximately equal contributions by HF and BO coupling in methane to mainly HT coupling in C_2H_6 and C_3H_8 (see Sec. IV).

(iii) The intensities of the vibrational substates of the C $1s^{-1}3p$ Rydberg state increase with increasing molecular size. This reflects the increasing variety of possible vibrations that can be simultaneously excited.

(iv) The energy separation between the lowest Rydberg state, the C $1s^{-1}3s$ resonance, and the higher Rydberg resonances, in particular the C $1s^{-1}3p$ resonance, increases from methane via ethane to propane. This is also reflected in the quantum defect, which is constant within the alkanes for C $1s^{-1}3p$ (0.77), but which decreases for the C $1s^{-1}3s$ excitation from methane (1.17) via ethane (1.10) to propane (1.05). This trend indicates that the screening of the nuclear potential is stronger in the larger molecules, where more screening electrons are available.

(v) All alkane molecules exhibit an increase in the energy of the C $1s^{-1}3s$ resonance upon deuteration.

ACKNOWLEDGMENTS

This work was supported by the Bundesminister für Forschung und Technologie, Project No. 05-5KEAXI-3/TP03. The authors gratefully acknowledge valuable discussions with D. A. Shirley, Pennsylvania State University, and E. Hudson, University of California at Berkeley, as well as expert assistance by the staff of BESSY.

[1] A. P. Hitchcock and I. Ishii, J. Electron Spectrosc. Relat. Phenom. **42**, 11 (1987).
[2] G. R. Wight and C. E. Brion, J. Electron Spectrosc. Relat. Phenom. **4**, 25 (1974).
[3] G. R. Wight and C. E. Brion, Chem. Phys. Lett. **26**, 607 (1974).
[4] A. P. Hitchcock, M. Pocock, and C. E. Brion, Chem. Phys. Lett. **49**, 125 (1977).
[5] M. Tronc, G. C. King, R. C. Bradford, and F. H. Read, J. Phys. B **9**, L555 (1976).
[6] M. Tronc, G. C. King, and F. H. Read, J. Phys. B **12**, 137 (1979).
[7] M. Domke, C. Xue, A. Puschmann, T. Mandel, E. Hudson, D. A. Shirley, and G. Kaindl, Chem. Phys. Lett. **173**, 122 (1990); **174**, 668 (1990).
[8] M. Domke, T. Mandel, A. Puschmann, C. Xue, D. A Shirley, and G. Kaindl, Rev. Sci. Instrum. **63**, 80 (1992).
[9] Y. Ma, C. T. Chen, G. Meigs, K. Randall, and F. Sette, Phys. Rev. A **44**, 1848 (1991).
[10] K. J. Randall, J. Feldhaus, W. Erlebach, A. M. Bradshaw, W. Eberhardt, Z. Xu, Y. Ma, and P. D. Johnson, Rev. Sci. Instrum. **63**, 1367 (1992).
[11] G. Remmers, M. Domke, A. Puschmann, T. Mandel, C. Xue, G. Kaindl, E. Hudson, and D. A. Shirley, Phys. Rev. A **46**, 3935 (1992).
[12] F. C. Brown, R. Z. Bachrach, and A. Bianconi, Chem. Phys. Lett. **54**, 425 (1978).
[13] W. Eberhardt, R.-P. Haelbich, M. Iwan, E. E. Koch, and C. Kunz, Chem. Phys. Lett. **40**, 180 (1976).
[14] P. S. Bagus, M. Krauss, and R. E. LaVilla, Chem. Phys. Lett. **23**, 13 (1973).
[15] J. W. Rabalais, T. Bergmark, L. O. Werme, L. Karlsson, and K. Siegbahn, Phys. Scr. **3**, 13 (1971).
[16] A. Koch and S. D. Peyerimhoff, Chem. Phys. Lett. **195**, 104 (1992).
[17] L. M. Sverdlov, M. A. Kovner, and E. P. Krainov, *Vibrational Spectra of Polyatomic Molecules* (Wiley, Jerusalem, 1974).
[18] G. Orlandi and W. Siebrand, Chem. Phys. Lett. **15**, 465 (1972).
[19] G. Herzberg, *Molecular Spectra and Molecular Structure,* Vol. 3 of Polyatomic Molecules (Van Nostrand, New York, 1966).
[20] L. S. Bartelli, K. Kuchitsa, and R. J. de Neui, J. Chem. Phys. **35**, 1211 (1961).
[21] D. L. Gray and A. G. Robiette, Mol. Phys. **37**, 1901 (1979).
[22] G. B. Sutherland and D. M. Dennison, Proc. R. Soc. London **148**, 250 (1935).
[23] P. A. Heimann, L. J. Medhurst, M. R. F. Siggel, D. A. Shirley, C. T. Chen, Y. Ma, and F. Sette, Chem. Phys. Lett. **183**, 234 (1991).